Environmental Science
Water Research & Technology

ROYAL SOCIETY OF CHEMISTRY

PAPER

View Article Online
View Journal | View Issue



Cite this: *Environ. Sci.: Water Res. Technol.*, 2025, **11**, 768

# Effect of inoculum percentage and hydrogen supply on hydrogenotrophic denitrification driven by anaerobic granular sludge†

Emanuele Marino, * Armando Oliva, Stefano Papirio, Giovanni Esposito and Francesco Pirozzi

Received 20th September 2024,
Accepted 3rd February 2025

DOI: 10.1039/d4ew00776j

rsc.li/es-water

Hydrogenotrophic denitrification ($H_2$Den) is an encouraging biological technology to remove nitrate ($NO_3^-$) from supply water with a low carbon/nitrogen ratio or in the absence of organic carbon. This study provides important insights into the use of anaerobic granular sludge for $NO_3^-$ removal from a synthetic water with an initial concentration of 200 mg $NO_3^-$ $L^{-1}$ (*i.e.*, 45.2 mg $NO_3^-$-N $L^{-1}$). This study investigated the effect of the inoculum input, expressed as percentage of reactor filling, *i.e.*, 10% *vs.* 20% *vs.* 40% (v/v) by the anaerobic granular sludge, as well as the hydrogen ($H_2$) supply, *i.e.*, stoichiometric *vs.* 50% excess *vs.* 100% excess, on the $H_2$Den process. Coupling 10% (v/v) inoculum percentage with 100% excess of $H_2$ supply was the most favourable condition, ensuring a $NO_3^-$ removal efficiency of up to 96%. Indeed, a 10% (v/v) inoculum percentage ensured the maximal denitrification rate, reaching 6.0 mg $NO_3^-$ $g^{-1}$ VS $d^{-1}$, which was further enhanced when increasing the $H_2$ dosage. Despite the great potential, this study also highlighted possible drawbacks of the anaerobic granular sludge-driven $H_2$Den process, such as nitrite ($NO_2^-$) accumulation as a denitrification intermediate. On the other hand, the release of gaseous denitrification intermediates such as $N_2O$ and NO was negligible under most of the investigated experimental conditions.

### Water impact

This study demonstrates the feasibility of using anaerobic granular sludge in hydrogenotrophic denitrification processes. Separation-based techniques for $NO_3^-$ removal from freshwaters are costly and environmentally impacting. Hydrogenotrophic denitrification driven by granular sludge is an attractive biological process that can be embedded into existing drinking water treatment plants as it facilitates the downstream separation steps and requires no chemical addition.

## 1 Introduction

Global freshwater reserves are in constant decline due to global population growth, industrialization, agricultural activities, and climate change correlated to droughts, storms, and floods. According to the report published by the Stockholm International Water Institute (SIWI) and UNICEF,[1] half the global population is expected to face freshwater scarcity in 25 years. Besides, inappropriate human activities cause the rapid deterioration of freshwater quality compromising the safe use of water.[2,3] Indeed, as a consequence of human alteration of the nitrogen (N) cycle, nitrate ($NO_3^-$) concentration in natural water is increasing worldwide.[4,5] The main anthropogenic causes for such alteration are the overuse of fertilizers in agricultural activities, uncontrolled municipal and industrial N-rich wastewater dumping, and explosives production for mining activities.[6–8] High $NO_3^-$ concentrations in drinking water can cause several diseases, such as gastric cancer, methemoglobinemia, and thyroid disorders.[3,9,10] Thus, the new EU Directive 2020/2184 on drinking water confirmed that $NO_3^-$ concentration shall not exceed 50 mg $L^{-1}$ in waters intended for human consumption.[11]

Different physical techniques have been employed for $NO_3^-$ removal from drinking water. The most widespread techniques are separation-based technologies such as reverse osmosis, ion exchange, electrochemical reduction, and activated carbon adsorption.[12] Besides having high application costs, some of these technologies, such as reverse osmosis and ion exchange, produce waste brine as a side product, which requires further treatments before discharging.[13] Biological denitrification represents a promising alternative to separation-based

*Department of Civil, Architectural and Environmental Engineering, University of Naples Federico II, Via Claudio 21, 80125, Naples, Italy.*
*E-mail: emanuele.marino@unina.it; Tel: +39 366 11 06 899*

† Electronic supplementary information (ESI) available. See DOI: https://doi.org/10.1039/d4ew00776j

techniques and is considered a less expensive and sustainable process compared to separation-based techniques.[14] Biological denitrification is an elimination-based technology aiming at $NO_3^-$ bioconversion to harmless nitrogen gas. Besides, studying the accumulation of denitrification intermediates is pivotal to fully understanding the biological denitrification process. For instance, nitrous oxide ($N_2O$) accumulation can be observed during biological denitrification, leading to the release of a well-known greenhouse gas with a 265 times higher global warming potential than carbon dioxide ($CO_2$), besides contributing to the stratospheric ozone depletion.[15,16]

Autotrophic denitrification (AuDen) is a promising biological process for $NO_3^-$ removal from drinking water, the latter being poor or totally lacking organic carbon. Indeed, applying the heterotrophic denitrification (HeDen) process for drinking water would require the supply of an external carbon source, serving as both the electron donor and carbon source. Besides being a further cost, an external carbon supply can lead to a larger sludge production and favour the presence of organic residues in the treated effluent.[17–19] On the other hand, AuDen exploits inorganic electron donors and inorganic carbon sources under anoxic conditions.[20] The most investigated electron donors for AuDen are reduced inorganic sulfur compounds, *e.g.*, elemental sulfur ($S^0$), sulfide ($S^{2-}$), thiosulfate ($S_2O_3^{2-}$), sulfite ($SO_3^{2-}$), and pyrite ($FeS_2$), thiocyanate ($SCN^-$), ferrous iron ($Fe^{2+}$), trivalent arsenic ($As^{3+}$), manganese (Mn), and hydrogen gas ($H_2$).[18,21] In particular, the use of $H_2$ is emerging due to its increased availability following the decarbonisation process pursued in the last decades. Indeed, green $H_2$ produced from renewable sources (*e.g.*, biomass fermentation and water splitting) is expected to overcome $H_2$ production from fossil fuels in the next few decades.[22] Moreover, using $H_2$ as an electron donor represents a valid alternative to conventionally utilized reduced inorganic sulfur compounds since it avoids sulfate formation. The stoichiometry of the hydrogenotrophic denitrification ($H_2$Den) reaction is reported in eqn (1):[18]

$$H_2 + 0.355\ NO_3^- + 0.049\ CO_2 + 0.355\ H^+ \rightarrow 0.010\ C_5H_7O_2N + 0.172\ N_2 + 1.143\ H_2O \quad (1)$$

$H_2$Den is a four-stage process in which $NO_3^-$ is step by step reduced to nitrite ($NO_2^-$), nitric oxide (NO), $N_2O$, and $N_2$ through reductase enzymes.[23] The use of $H_2$ as electron donor showed several advantages over other substances, such as i) no production of toxic by-products, ii) high $NO_3^-$ removal efficiency, iii) low biomass yield (*i.e.*, 0.23 g cells per g $NO_3^-$) meaning low sludge production, iv) cost-effectiveness (*i.e.*, 0.41 kg $H_2$/kg $NO_3^-$), and v) no downstream operations required to remove the electron donor in excess.[13,18] Besides the benefits, using $H_2$ presents some drawbacks, such as the low $H_2$ solubility, which results in limited gas–liquid mass transfer, and handling issues in terms of safety.[24]

The present study investigated the implementation of anaerobic granular sludge (AnGS) in the $H_2$Den process, studying the impact of inoculum percentage (v/v) and $H_2$ supply on the $H_2$Den performance. AnGS is commonly employed in fermentative and anammox processes.[25,26] To the best of the authors' knowledge, AnGS application in the $H_2$Den process has been explored in only a limited number of studies, highlighting its potential as an innovative alternative to traditional suspended-cell and attached-growth systems.[20,27,28] Using microorganisms in granular form for $H_2$Den can offer several distinct advantages. AnGS enhances the process stability even under challenging conditions such as low temperature and the presence of inhibitors. Furthermore, the compact structure and high density of the granular sludge promote greater $NO_3^-$ removal and higher biomass concentrations compared to attached-growth systems.[20] In particular, this is the first study focusing on investigating the effect of the inoculum percentage (v/v) in AuDen, with neither an AnGS nor traditional sludges being previously investigated in this perspective for drinking water treatment. The reduced use of the sludge could make the process more attractive for drinking water production plants, facilitating the downstream separation of microorganisms from water intended for human consumption. Furthermore, different from the few studies available in the literature on the AnGS $H_2$Den process,[20,27] no external inorganic carbon source was added in this study. Indeed, tap water was used as the background solution during the experiments to exploit the inorganic carbon naturally present in tap water, representing an additional saving in terms of chemicals employed. To elucidate the potential of the AnGS $H_2$Den process and highlight the possible drawbacks, $NO_3^-$ and $NO_2^-$ concentration trends and the composition of gas produced at the end of the process were monitored.

# 2 Materials and methods

## 2.1 Synthetic water, electron donor and inoculum

Three solutions (S) were prepared for the experimental activity. S1 consisted of 0.362 g $L^{-1}$ of $KNO_3$ as nitrate source, 0.123 g $L^{-1}$ of $NaH_2PO_4{\cdot}2H_2O$ and 0.360 g $L^{-1}$ of $K_2HPO_4{\cdot}3H_2O$ as buffers.[20] S2 was prepared ensuring a concentration of 0.407, 0.138, and 0.405 g $L^{-1}$ of $KNO_3$, $NaH_2PO_4{\cdot}2H_2O$, and $K_2HPO_4{\cdot}3H_2O$, respectively. S3 was made up of 0.543 g $L^{-1}$ of $KNO_3$, 0.184 g $L^{-1}$ of $NaH_2PO_4{\cdot}2H_2O$ and 0.540 g $L^{-1}$ of $K_2HPO_4{\cdot}3H_2O$. The inorganic carbon source was provided using tap water with a 0.38 g $CaCO_3$/L alkalinity as the background to prepare all solutions. $H_2$, serving as the electron donor, was produced using a F11-HHO hydrogen dry cell (Hydrobullet Hydrogen Technology, Athens, Greece). An AnGS was used as the source of microorganisms. The AnGS was collected from a dairy wastewater treatment plant (Kilconnell, Ireland) and stored at 4 °C before use. The characteristics of the AnGS were previously reported by Oliva *et al.*,[29] who used the same inoculum.

## 2.2 Chemicals

Potassium nitrate ($KNO_3$, purity ≥ 99.0%) was provided by Sigma-Aldrich (Steinheim, Germany). Sodium phosphate monobasic trihydrate ($NaH_2PO_4{\cdot}2H_2O$, purity ≥ 98.0%) was

furnished by J.T. Baker (Milan, Italy). Di-Potassium hydrogen phosphate trihydrate ($K_2HPO_4 \cdot 3H_2O$, purity ≥ 99.0%) was provided by ITW Reagents (Monza, Italy).

### 2.3 Experimental conditions

Two sets of $H_2$Den tests were performed (Table 1). The first set of tests investigated the impact of inoculum percentage (v/v) on denitrification. The I10, I20 and I40 tests were prepared filling, respectively, 10, 20, and 40% (v/v) of the working volume ($V_{work}$) with AnGS and the remaining $V_{work}$ with S1, S2, and S3, respectively (Table 1). Thus, all bottles were prepared ensuring an initial concentration of 200 mg $NO_3^-$ $L^{-1}$ (*i.e.*, 45.2 mg $NO_3^-$-N $L^{-1}$). The initial $NO_3^-$ concentration was chosen based on the nitrate concentration values found in some natural environments. Indeed, Abascal *et al.*[5] reported that in some regions of the world, *i.e.*, in Asia, the $NO_3^-$ concentration reached a value fourfold higher than 50 mg $L^{-1}$, which is the standard recommended by the World Health Organization. In I10, I20 and I40, $H_2$ was provided 50% in excess compared to the stoichiometry.[18] The second set of experiments was performed by varying the $H_2$ supply, *i.e.*, stoichiometric (Hst), 50% in excess (H50), and 100% in excess (H100) (Table 1). In the second set, the inoculum percentage was maintained at 10% (v/v), filling the remaining $V_{work}$ with S1. In addition to the two sets of $H_2$Den tests, two controls were performed. The first control, *i.e.* an abiotic control (AC), investigated whether $NO_3^-$ removal occurred in the absence of inoculum without varying pH and temperature (Fig. S1 – ESI† material). Besides, the second control, *i.e.* C10, C20, and C40 for the first set and C for the second set of experiments (Table 1), was carried out to investigate whether the organic substances potentially originating from cell death and cell lysis could contribute to $NO_3^-$ removal, by acting as an organic electron donor, in the absence of $H_2$ at different inoculum percentages.[30]

### 2.4 Experimental setup

The experimental tests were carried out in 250 mL serum glass bottles (OCHS, Lenglern, Germany) (Fig. 1). The bottles were filled with synthetic solutions and AnGS, reaching a $V_{work}$ of 125 mL (Table 1). A trace metal solution (1 mL $L^{-1}$), prepared as described by Wang *et al.*,[20] was added to each bottle. Before starting the experiments, argon gas (Ar) was used to flush the bottles from the bottom and ensure dissolved oxygen removal and anoxic condition in the headspace. The bottles were then vented to atmospheric pressure. $H_2$ was added to the headspace volume in the $H_2$Den tests (Table 1). In control tests (Table 1), $H_2$ was replaced by extra Ar to ensure the same starting pressure in all bottles. The initial pH was adjusted to 8.0 ± 0.2 using a 3 M KOH solution to ensure optimal pH conditions for the $H_2$Den process.[18] After sealing each serum bottle with a rubber septum and aluminium crimp, a needle equipped with 1-way stopcocks (Masterflex, Gelsenkirchen, Germany) for gas and liquid sampling was inserted in the rubber septum. The bottles were operated at room temperature, *i.e.*, between 18.8 and 20.7 °C, and continuously shaken at 70 rpm using a SM 30 Universal Shaker (Edmund Buhler, Bodelshausen, Germany). All experiments were performed in triplicate.

For each experimental condition, 6 days of batch experiments were repeated 3 times to ensure the reproducibility of the experiments. In both sets, the AnGS used for the triplicate of each condition was mixed after any cycle and used to prepare the triplicate in the following cycle under the same condition. Between the two sets of experiments, all the AnGS used in the first set (*i.e.*, from I10, I20, I40, and control tests) was collected from the bottles, mixed manually and equally divided among the bottles used in the second set (*i.e.*, Hst, H50, H100, and controls). Liquid samples were collected fourfold during the experiments (*i.e.*, on days 0, 1, 3, and 6) and filtered through a 0.45 μm polypropylene syringe filter (VWR, Milan, Italy) before analysis. The headspace was sampled at the end of each cycle to evaluate the gaseous composition after the $H_2$Den process.

### 2.5 Analytical methods

$NO_3^-$ and $NO_2^-$ were measured by a 761 compact ion chromatograph (Metrohm, Herisau, Switzerland) equipped

**Table 1** Experimental design

| Test | ID test | Solutions (S) input (mL) | Inoculum percentage[a] (v/v) | Volume of $H_2$ supplied (mL) | Volume of $H_2O$ added (mL) |
|---|---|---|---|---|---|
| Abiotic control | AC | 100 of S2 | — | 42.1 (excess of 50%) | 25 |
| | AC-st | 112.5 of S1 | — | 28.1 (stoichiometric) | 12.5 |
| | AC-50 | | | 42.1 (excess of 50%) | |
| | AC-100 | | | 56.1 (excess of 100%) | |
| Inoculum percentage | I10 | 112.5 of S1 | 10% (0.65 g VS) | 42.1 (excess of 50%) | — |
| | I20 | 100 of S2 | 20% (1.30 g VS) | | |
| | I40 | 75 of S3 | 40% (2.60 g VS) | | |
| $H_2$ supply | Hst | 112.5 of S1 | 10% (0.65 g VS) | 28.1 (stoichiometric) | — |
| | H50 | | 10% (0.65 g VS) | 42.1 (excess of 50%) | |
| | H100 | | 10% (0.65 g VS) | 56.1 (excess of 100%) | |
| Controls | C10 | 112.5 of S1 | 10% (0.65 g VS) | — | — |
| | C20 | 100 of S2 | 20% (1.30 g VS) | | |
| | C40 | 75 of S3 | 40% (2.60 g VS) | | |
| | C | 112.5 of S1 | 10% (0.65 g VS) | | |

[a] Grams of volatile solids (g VS) were based on the characteristics reported by Oliva *et al.*,[29] who used the same inoculum.

 

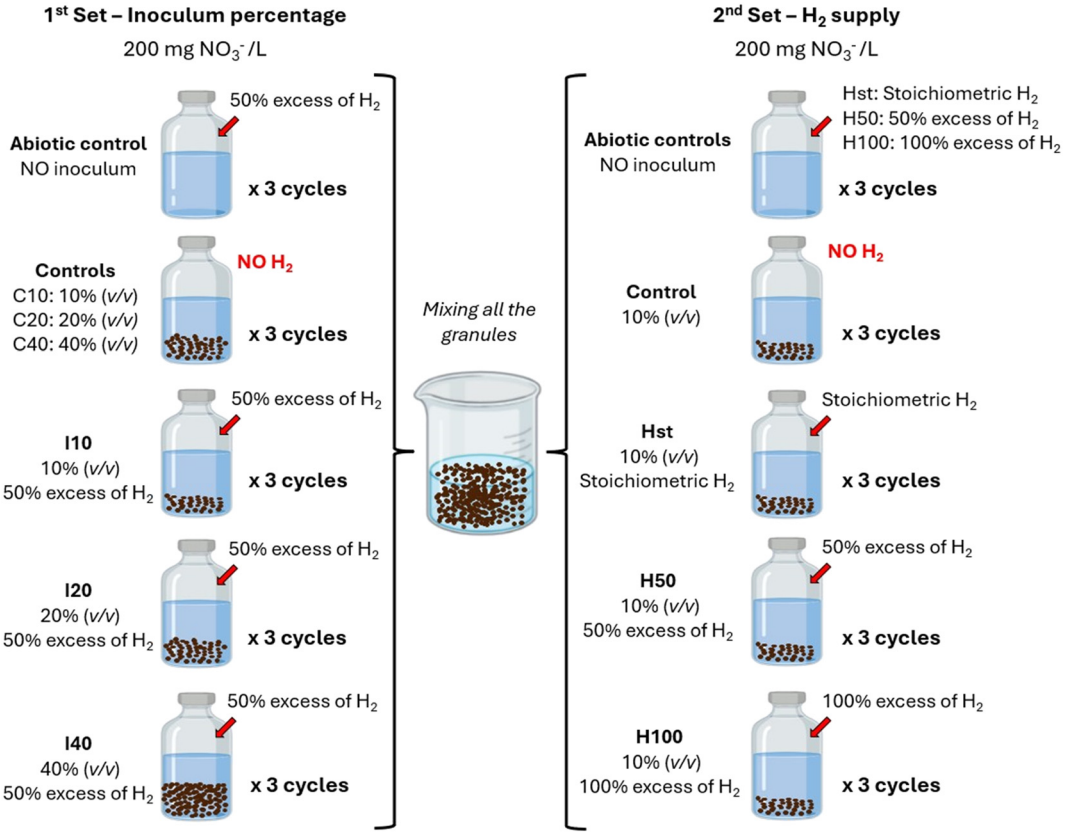


**Fig. 1** Schematic of the experimental tests carried out in 250 ml serum glass bottles.

with an IonPac AS12A anionic column (with a detection limit of 0.05 mg $L^{-1}$ for $NO_3^-$ and $NO_2^-$) (Dionex, Waltham, USA), as described by Di Capua *et al.*[31] The pH was measured at each liquid sampling using a HI98100 Checker Plus pH meter (Hanna Instrument, Padova, Italy). Organic carbon, inorganic carbon and total carbon of the soluble fraction filtered at 0.45 μm were measured using a TOC-$L_{CSN}$ analyser (Shimadzu, Kyoto, Japan). Briefly, the samples were treated in a combustion chamber at a temperature of 680 °C in the presence of a catalyst. The instrument, equipped with a non-dispersive infrared sensor (NDIR) detector, utilizes oxygen ($O_2$) as carrier gas at a flow rate of 150 mL $min^{-1}$. The headspace pressure was monitored regularly with a Leo 1 pressure meter (Keller, Winterthur, Switzerland). The headspace composition at the end of the batch tests was evaluated using a HPR-20 R&D mass spectrometer (Hiden Analytical, Warrington, UK), as described by Oliva *et al.*[32] The mass spectrometer used a Faraday Cup as the detector with the lower limit of 1 ppm to detect $H_2$, methane ($CH_4$), $CO_2$, water vapour ($H_2O_{(g)}$), NO, $N_2O$, $N_2$, $O_2$, and Ar.

### 2.6 Calculations

The $NO_3^-$ removal efficiency (NRE) at a certain day was calculated following eqn (2):

$$\mathrm{NRE} = \frac{[\mathrm{NO_3^-}]_{in} - [\mathrm{NO_3^-}]_i}{[\mathrm{NO_3^-}]_{in}} \cdot 100 \quad (2)$$

where $[NO_3^-]_{in}$ is the $NO_3^-$ concentration measured on day 0 and $[NO_3^-]_i$ is the $NO_3^-$ concentration on a certain day of the test ($i$ = 1, 3, and 6).

The specific denitrification rate was calculated following eqn (3) and expressed in mg $NO_3^-$ $g^{-1}$ VS $d^{-1}$.

$$\text{Specific denitrification rate} = \frac{\left([\mathrm{NO_3^-}]_i - [\mathrm{NO_3^-}]_j\right) \cdot V_{work}}{\Delta t \cdot \mathrm{VS}} \quad (3)$$

where $[NO_3^-]_i$ is the $NO_3^-$ concentration at a certain day of the test ($i$ = 0, 1, 3 and 6 days) and $[NO_3^-]_j$ is the $NO_3^-$ concentration measured on the following sampling day. VS represents the grams of volatile solids (g VS) used in each condition. The time interval $\Delta t$ is equal to the difference between the two sampling days considered in the calculation. The specific denitrification rate was also evaluated by considering the difference between the $NO_3^-$ concentration on day 0 ($i$ = 0) and day 6 ($j$ = 6). The overall specific denitrification rate was then calculated by averaging the values obtained in the three cycles for each experimental condition.

The difference in $NO_3^-$ concentration on a certain day between two tests was calculated following eqn (4) and expressed in mg $NO_3^-$ $L^{-1}$.

$$\text{Difference in } \mathrm{NO_3^-} \text{ concentration} = ([\mathrm{NO_3^-}]_i)_A - ([\mathrm{NO_3^-}]_i)_B \quad (4)$$

where $[NO_3^-]_i$ is the $NO_3^-$ concentration at a certain day of the test ($i$ = 0, 1, 3 and 6 days), whereas A and B generically represent two different tests.

### 2.7 Statistical comparison

The results achieved under the different experimental conditions were compared with the related control test using the Minitab 21 Statistical Software (Minitab LCC, Pennsylvania, USA). In the first set of experiments, $NO_3^-$ concentrations in I10, I20 and I40 were individually compared with the $NO_3^-$ concentrations of the corresponding control test (*i.e.*, C10, C20, and C40). In the second set of experiments, $NO_3^-$ concentrations in Hst, H50 and H100 were compared with the sole control test available (C), and between each other. A one-way analysis of variance (ANOVA) followed by the Tukey *post hoc* test was performed. The difference was considered statistically significant when the $p$-value was below 0.05.

## 3 Results and discussion

### 3.1 Effect of inoculum percentage (v/v) on hydrogenotrophic denitrification

$NO_3^-$ and $NO_2^-$ concentration trends at varying inoculum percentages are given in Fig. 2. The $NO_3^-$ concentration trend (Fig. 2A, C and E) shows that the difference in $NO_3^-$

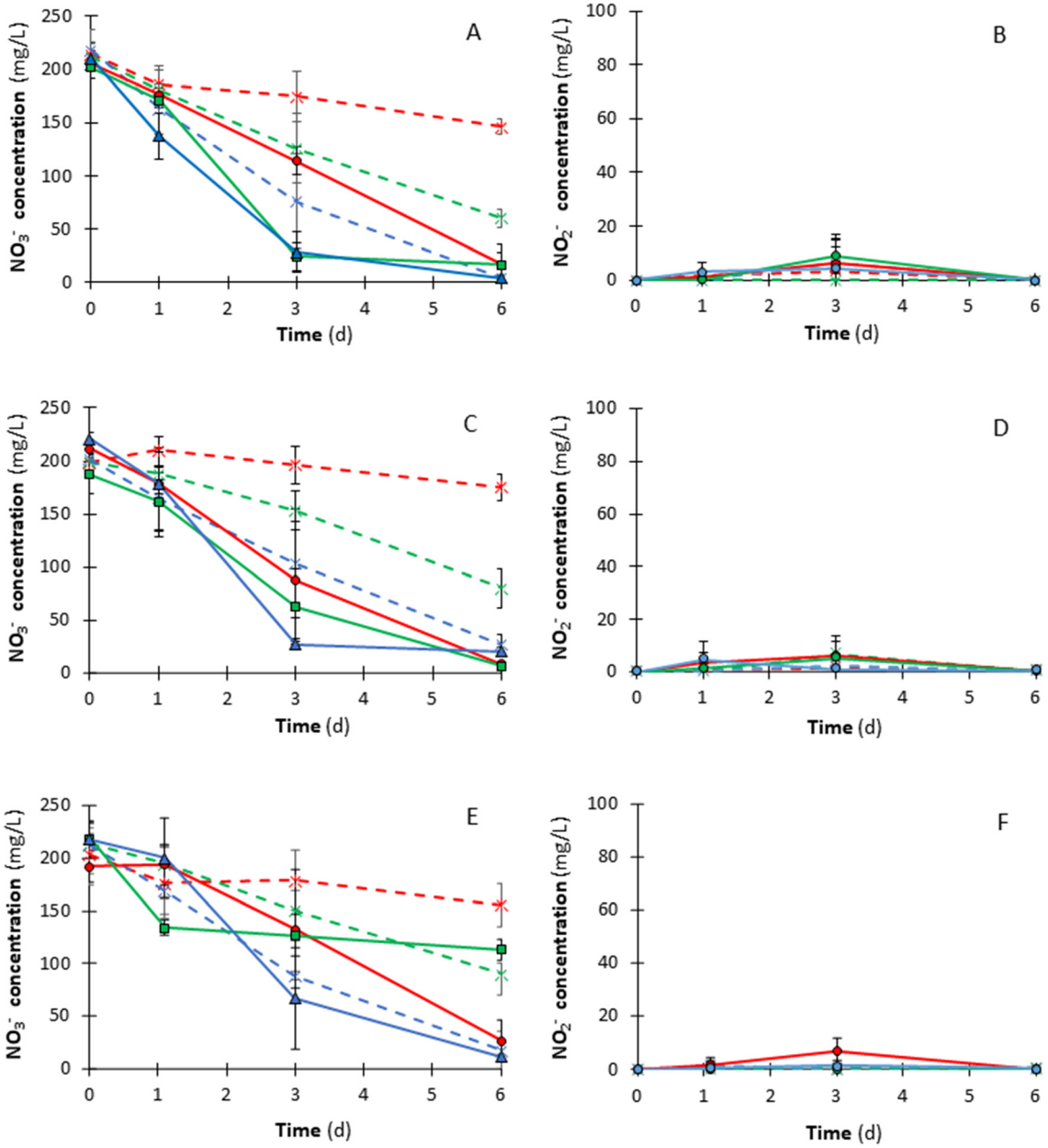


Fig. 2 Nitrate ($NO_3^-$) (left column) and nitrite ($NO_2^-$) (right column) concentration trend during the hydrogenotrophic denitrification tests across three cycles: the first cycle (A and B), second cycle (C and D), and third cycle (E and F). The tests were conducted using different inoculum percentages, *i.e.*, 10% (I10), 20% (I20) and 40% (I40) (v/v). Inoculum percentage tests: I10 (●), I20 (■), I40 (▲). Control tests: C10 (×), C20 (×), C40 (×).

 

concentration between the experimental condition (*i.e.*, I10, I20, and I40) and the corresponding control test (*i.e.*, C10, C20, and C40) increased when the inoculum percentage was low, *i.e.*, 10% (v/v). This behaviour was evident at the end of the experiment, *i.e.*, on day 6, when, for each cycle, the highest difference in $NO_3^-$ concentration was observed between I10 and C10 (Fig. 2A, C and E). The difference in $NO_3^-$ concentration between I10 and C10 was 129.7 mg $NO_3^-$ $L^{-1}$ (*i.e.*, 29.3 mg $NO_3^-$-N $L^{-1}$) for the 1st cycle, 166.5 mg $NO_3^-$ $L^{-1}$ (*i.e.*, 37.6 mg $NO_3^-$-N $L^{-1}$) for the 2nd cycle and 128.4 mg $NO_3^-$ $L^{-1}$ (*i.e.*, 29.0 mg $NO_3^-$-N $L^{-1}$) for the 3rd cycle. For instance, in the 2nd cycle, on day 6, the residual $NO_3^-$ concentration was 8.8 mg $NO_3^-$ $L^{-1}$ (*i.e.*, 2.0 mg $NO_3^-$-N $L^{-1}$) for I10 and 175.3 mg $NO_3^-$ $L^{-1}$ (*i.e.*, 39.6 mg $NO_3^-$-N $L^{-1}$) for C10 (Fig. 2C), indicating that a great part of the fed $NO_3^-$ was removed by $H_2$Den. Since each solution did not contain organic electron donors, the organic substance used to remove $NO_3^-$ in the control tests was likely released from the AnGS after cell death and lysis. Indeed, the intracellularly stored organic matter of AnGS microorganisms can be used for endogenous HeDen as a source of carbon and energy.[33]

On day 6, the difference in $NO_3^-$ concentration between I20 and C20 ($p < 0.05$) and between I40 and C40 ($p > 0.05$) were lower than that between I10 and C10 ($p < 0.05$) (Table 2). In the 2nd cycle, the residual $NO_3^-$ concentration was 7.2 mg $NO_3^-$ $L^{-1}$ (*i.e.*, 1.6 mg $NO_3^-$-N $L^{-1}$) for I20 and 80.6 mg $NO_3^-$ $L^{-1}$ (*i.e.*, 18.2 mg $NO_3^-$-N $L^{-1}$) for C20, whereas the residual $NO_3^-$ concentration was 20.5 mg $NO_3^-$ $L^{-1}$ (*i.e.*, 4.6 mg $NO_3^-$-N $L^{-1}$) for I40 and 27.0 mg $NO_3^-$ $L^{-1}$ (*i.e.*, 6.1 mg $NO_3^-$-N $L^{-1}$) for C40 (Fig. 2C). Thus, experimental tests and controls reached about the same residual $NO_3^-$ concentration at the end of tests when the inoculum percentage was 40% (v/v) (Fig. 2), with an NRE of 98.2% in the first cycle. These results confirm that mixotrophic denitrification likely occurred and that the endogenous HeDen denitrification rate was higher with increased inoculum percentages (v/v) (Fig. 2). Similarly, Chang *et al.*[34] observed the co-existence of sulfur-based autotrophic denitrification and endogenous denitrification in a sulfur-based fiber carrier fixed-bed reactor. Thus, a 10% (v/v) inoculum percentage could favour the hydrogenotrophic pathway against the heterotrophic one. Furthermore, a 10% (v/v) inoculum percentage ensured the maximum average specific denitrification rate of 6.0 mg $NO_3^-$ $g^{-1}$ VS $d^{-1}$, calculated over the entire duration of the tests (Table 2). In the corresponding control test (*i.e.* C10), the average specific denitrification rate was only 1.5 mg $NO_3^-$ $g^{-1}$ VS $d^{-1}$, suggesting a great impact of $H_2$ supply at low AnGS percentages. In contrast, for I20 and I40, the average specific denitrification rate (2.5 and 1.6 mg $g^{-1}$ VS $d^{-1}$, respectively) was similar to the control tests, *i.e.*, 2.1 mg $NO_3^-$ $g^{-1}$ VS $d^{-1}$ for C20 and 1.6 mg $NO_3^-$ $g^{-1}$ VS $d^{-1}$ for C40 (Table 2).

Fig. 2 shows that increasing the inoculum percentage up to 40% (v/v) allowed to meet the $NO_3^-$-N regulatory limit for drinking water (*i.e.*, 11.3 mg $L^{-1}$) already after 3 days of operation. In contrast, a 10% (v/v) inoculum percentage did not favour a quick start-up of denitrification, as per the NRE

**Table 2** Nitrate ($NO_3^-$) removal efficiency (NRE) and specific denitrification rate (SDR) in the inoculum percentage tests and the corresponding controls accompanied by statistical information (SI) referring to the residual $NO_3^-$ concentration

| Cycle | Time (d) | NRE (%) | | SDR (mg $NO_3^-$ $g^{-1}$ VS $d^{-1}$) | | Statistical Information[a] | NRE (%) | | SDR (mg $NO_3^-$ $g^{-1}$ VS $d^{-1}$) | | Statistical Information[a] | NRE (%) | | SDR (mg $NO_3^-$ $g^{-1}$ VS $d^{-1}$) | | Statistical Information[a] |
|---|---|---|---|---|---|---|---|---|---|---|---|---|---|---|---|---|
| | | C10 | I10 | C10 | I10 | C10 *vs.* I10 | C20 | I20 | C20 | I20 | C20 *vs.* I20 | C40 | I40 | C40 | I40 | C40 *vs.* I40 |
| 1st | 1 | 13.0 | 14.1 | 5.4 | 5.6 | a – a | 14.6 | 15.2 | 3.0 | 3.0 | a – a | 25.4 | 34.6 | 2.1 | 3.5 | a – a |
| | 3 | 18.3 | 44.2 | 1.1 | 5.9 | a – b | 40.4 | 88.1 | 2.6 | 7.1 | a – b | 65.1 | 86.5 | 1.9 | 2.6 | a – a |
| | 6 | 31.7 | 91.9 | 1.8 | 6.3 | a – b | 71.6 | 91.8 | 2.1 | 0.2 | a – b | 98.3 | 98.2 | 1.1 | 0.4 | a – a |
| 2nd | 1 | 0.0 | 15.6 | 0.0 | 6.3 | a – a | 5.4 | 13.5 | 1.0 | 2.4 | a – a | 18.2 | 19.0 | 1.8 | 2.0 | a – a |
| | 3 | 1.1 | 58.5 | 1.3 | 8.7 | a – b | 22.8 | 66.5 | 1.7 | 4.8 | a – b | 48.7 | 87.8 | 1.5 | 3.6 | a – a |
| | 6 | 11.7 | 95.8 | 1.4 | 5.1 | a – b | 59.5 | 96.2 | 2.3 | 1.8 | a – b | 86.6 | 90.7 | 1.2 | 0.1 | a – a |
| 3rd | 1 | 13.3 | 0.0 | 5.2 | 0.0 | a – a | 8.5 | 38.6 | 1.7 | 8.1 | a – b | 20.5 | 8.3 | 2.1 | 0.9 | a – a |
| | 3 | 12.2 | 31.0 | 0.0 | 5.9 | a – a | 29.3 | 42.0 | 2.1 | 0.4 | a – a | 58.2 | 69.1 | 1.9 | 3.2 | a – a |
| | 6 | 23.6 | 85.9 | 1.5 | 6.8 | a – b | 57.5 | 47.9 | 1.9 | 0.4 | a – b | 91.5 | 94.6 | 1.1 | 0.9 | a – a |
| Mean SDR[b] | | | | 1.5 | 6.0 | | | | 2.1 | 2.5 | | | | 1.6 | 1.6 | |

[a] Significant difference (*i.e.*, $p < 0.05$) occurs when two conditions do not share letters (*e.g.*, a – b). [b] The mean SDR was calculated over the 6 days of operation as an average of the three experimental cycles.

values reported in Table 2. The enhanced rate of $NO_3^-$ removal observed in I40 tests was likely due to the dominant contribution of the endogenous heterotrophic pathway, which was favoured at higher inoculum percentages. Indeed, HeDen kinetics are notably faster than AuDen.[35] On day 1, for the I10 condition and the corresponding control C10, the highest NRE observed was 15.6%, whereas the NRE of I40 and C40 was about 20% in the second cycle (Table 2). From day 3 onwards, in all cycles, the NRE was constantly higher than in the corresponding control tests, regardless of the inoculum percentage (Table 2). For instance, in the first cycle, the NRE was 86.5% for I40 and 65.1% for C40. Whereas, on day 6, the difference in terms of NRE between C10 and I10 confirmed that the hydrogenotrophic metabolism was likely favoured at low biomass percentages (Table 2).

At the end of the experiment, the residual $NO_3^-$ concentration was constantly below the regulatory limit of 50 mg $L^{-1}$ for drinking water,[9] except for the 3rd cycle of the I20 test, in which the $NO_3^-$ concentration on day 6 was 113.6 mg $L^{-1}$ (*i.e.*, 25.7 mg $NO_3^-$-N $L^{-1}$), which corresponds to a 47.9% NRE (Fig. 2). This trend suggests that, under the experimental conditions tested in the present study, an increase in the number of cycles does not necessarily correspond to an improvement in process efficiency. A possible explanation is that three cycles were not perhaps sufficient to properly acclimate the granules under $H_2$Den conditions. Also, the occurrence of shear forces between the granules generated while continuously shaking the bottles at 70 rpm could cause cell erosion and disaggregation, ultimately reducing the process performance and hindering $NO_3^-$ removal.[36] Such consideration can be supported by the organic carbon measurements (Table S3 – ESI† material), showing that the available solubilised organic carbon observed at the end of each cycle decreased as the number of cycles increased. Therefore, the release of organic matter from AnGS was higher at the start of the experimental tests, thus the endogenous HeDen contribution in $NO_3^-$ removal was likely higher in the 1st cycle.

As regards $NO_2^-$ (Fig. 2B, D and F), the mean $NO_2^-$ concentration was constantly below the regulatory limit of 0.50 mg $L^{-1}$ (*i.e.*, 0.15 mg $NO_2^-$-N $L^{-1}$)[11] at the end of tests except for controls C10 and C20 in the 3rd cycle, in which residual $NO_2^-$ concentration was 0.57 and 0.58 mg $L^{-1}$ (*i.e.*, 0.17 and 0.18 mg $NO_2^-$-N $L^{-1}$), respectively. Nevertheless, $NO_2^-$ accumulation was observed on days 1 and 3, revealing the presence of intermediates in the liquid phase during the process. On day 3, the highest $NO_2^-$ concentration was 9.10 mg $L^{-1}$ (*i.e.*, 2.77 mg $NO_2^-$-N $L^{-1}$) in the 2nd cycle for I20. This trend suggests that further time is required to reduce $NO_2^-$ when $NO_3^-$ is the sole electron acceptor and when $H_2$ is the main electron donor. $NO_2^-$ accumulation could be due to the competition for $H_2$ between $NO_3^-$ reductase and $NO_2^-$ reductase.[27] It must be noted that, in the present study, $H_2$ was supplied only at the start of each batch test. Therefore, the electron donor availability could become a limiting factor in the intermediate days, favouring the competition between $NO_2^-$ and $NO_3^-$reductases. A similar $NO_2^-$ concentration trend was reported by Wang *et al.*[37] using $S^{2-}$ as the electron donor. Indeed, the $NO_2^-$ concentration decreased when the available $NO_3^-$ was entirely consumed, revealing that $NO_3^-$ is a more favoured electron acceptor than $NO_2^-$.

### 3.2 Impact of hydrogen supply on denitrification performance

The second set of experiments investigated the impact of different $H_2$ supplies, *i.e.*, stoichiometric *vs.* 50% in excess *vs.* 100% in excess, on the $H_2$Den process. $NO_3^-$ and $NO_2^-$ concentration trends are given in Fig. 3. The $NO_3^-$ concentration trend showed that the difference in $NO_3^-$ concentration between the $H_2$ supply tests and the control increased when increasing the $H_2$ supply (Fig. 3A, C and E). Similarly, Li *et al.*[27] recently observed that using a granular sludge as the inoculum and increasing the dissolved hydrogen concentration from 0.02 to 0.40 mg $L^{-1}$ (corresponding to $H_2$ percentages in the headspace of 10 and 100%, respectively), the $NO_3^-$-N removal rate gradually increased from 0.25 to 0.66 mg $NO_3^-$-N $mg^{-1}$ MLSS $d^{-1}$. In the present study, on day 6, the difference in $NO_3^-$ concentrations between Hst, H50 and H100 tests and the control test was respectively 60.7, 65.8, and 69.4 mg $NO_3^-$ $L^{-1}$ (*i.e.*, 13.7, 14.9, and 15.7 mg $NO_3^-$-N $L^{-1}$) in the 1st cycle. The difference in $NO_3^-$ concentrations was respectively equal to 71.5, 78.4, and 79.3 mg $NO_3^-$ $L^{-1}$ (*i.e.*, 16.1, 17.7, and 17.9 mg $NO_3^-$-N $L^{-1}$) in the 2nd cycle and 42.0, 54.5, and 65.4 mg $NO_3^-$ $L^{-1}$ (*i.e.*, 9.5, 12.3, and 14.8 mg $NO_3^-$-N $L^{-1}$) in the 3rd cycle. Thus, all results of $H_2$ supply tests were significantly ($p < 0.05$) different from the control test in terms of residual $NO_3^-$ concentration in all cycles (Table 3). Nevertheless, all investigated $H_2$ supplies led to similar ($p > 0.05$) NRE at the end of the process (Table 3). Indeed, the average specific denitrification rate evaluated over the entire duration of tests was similar for each condition, being recorded at 5.3, 5.6 and 5.8 mg $NO_3^-$ $g^{-1}$ VS $d^{-1}$ respectively for Hst, H50 and H100 (Table 2). On the other hand, the control test reached the value of 3.3 mg $NO_3^-$ $g^{-1}$ VS $d^{-1}$.

In particular, the highest NRE, *i.e.*, 95.3%, was reached in the H100 tests in the 2nd cycle, as shown in Table 3. On day 3, instead, the difference in $NO_3^-$ concentration between the Hst test and H50 and H100 increased while increasing the number of cycles (Fig. 3A, C and E), suggesting that a stoichiometric $H_2$ supply is not sufficient to enhance the $NO_3^-$ removal rate, likely due to the limited availability of the inorganic electron donor.[38]

Besides, comparing the two sets of experiments, likely a higher number of cycles would have been beneficial to appreciate the adaption of the microorganisms.[39] In support of this hypothesis, it was observed that even if I10 and H50 tests were performed under the same experimental conditions, they did not return the same concentration trend (Fig. 2 and 3). Indeed, both conditions have similar NREs at the end of the tests, but for H50 higher NREs were

 

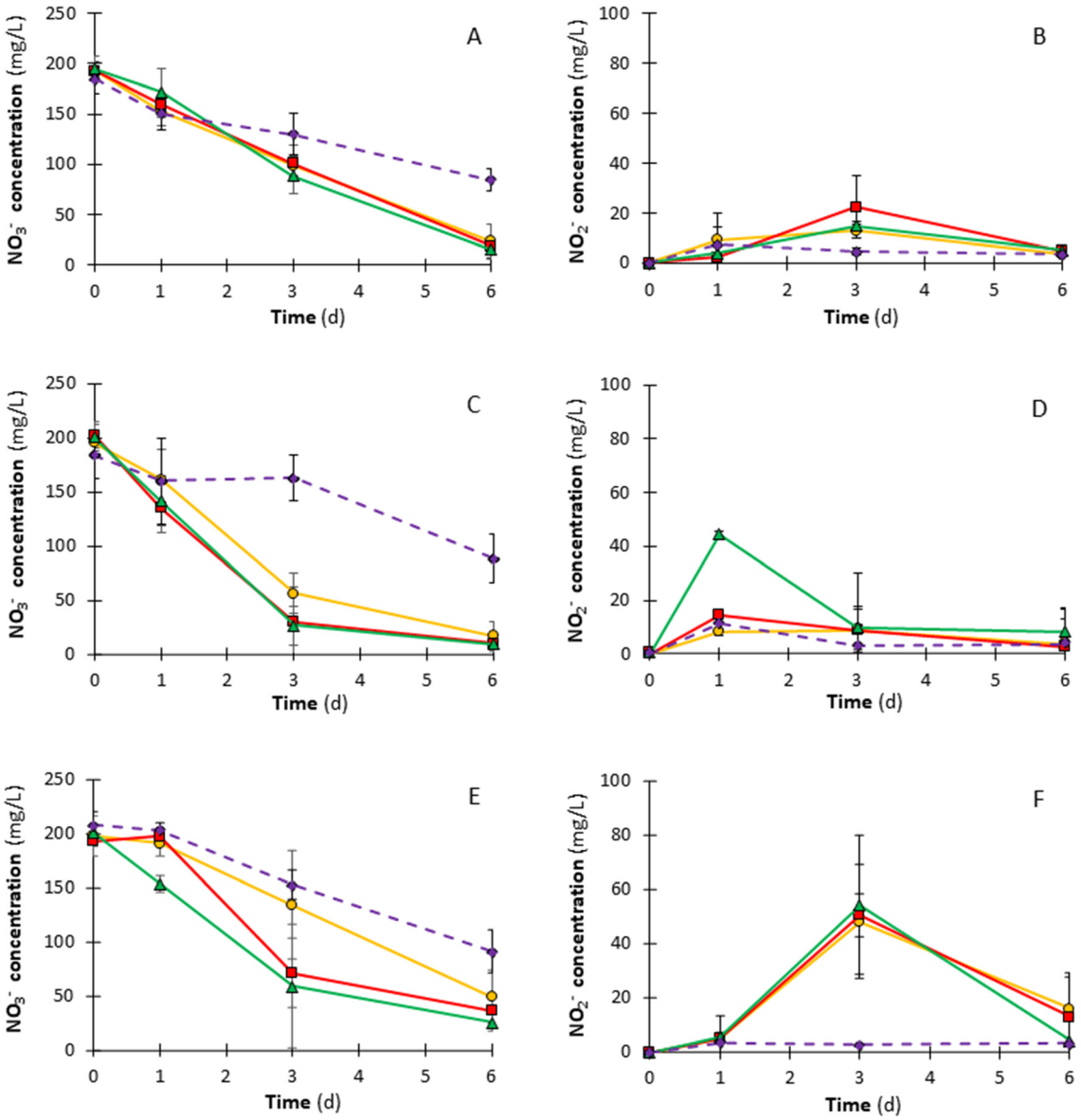


Fig. 3 Nitrate ($NO_3^-$) (left column) and nitrite ($NO_2^-$) (right column) concentration trend during the hydrogenotrophic denitrification tests across three cycles: the first cycle (A and B), second cycle (C and D), and third cycle (E and F). The tests were conducted varying the hydrogen supply, *i.e.*, stoichiometric (Hst), 50% in excess (H50), and 100% in excess (H100). Hydrogen supply tests: Hst (●), H50 (■), H100 (▲). Control test with 10% (v/v) inoculum percentage and in the absence of hydrogen supply: C (◆).

reached on day 3 respect to I10. Thus, likely, a longer biomass acclimatization enhanced the AnGS $H_2$Den rate. In addition, the disruption of the AnGS may have increased in the second set of experiments due to the overall increased exposure to the shearing forces generated while shaking the bottles, resulting in increased organic matter release from the granules, as also supported by the organic carbon measurements (Table S3 – ESI† material). For instance, in the first cycle for Hst, organic carbon was not detected on day 0, while it was equal to 65.4 mg $L^{-1}$ on day 6. This hypothesis is also supported by the difference between the controls C10 (first set of tests) and C (second set of tests), which were prepared following the same recipe (Table 1) but resulted in different NREs (Tables 2 and 3). The release of organic matter from the granules can be further limited by implementing a reactor configuration that maintains granules in their original shape by limiting cell erosion and disaggregation, *e.g.*, an upflow anaerobic sludge blanket (UASB) reactor.

Fig. 3 shows that after a significant $NO_2^-$ accumulation in the intermediate days, the residual $NO_2^-$ concentration decreased at the end of each test. Nevertheless, the final $NO_2^-$-N concentration (*i.e.*, 4.90 mg $NO_2^-$-N $L^{-1}$ at worst) suggests that the process was not yet completed after 6 days. Indeed, in the 3rd cycle, $NO_2^-$ accumulation was higher than in the other two cycles, except for H100, in

**Table 3** Nitrate removal efficiency (NRE) and specific denitrification rate (SDR) in the hydrogen supply tests and the corresponding controls accompanied by statistical information (SI) referring to the residual nitrate concentration

| | | NRE (%) | | | | SDR (mg $NO_3^-$ $g^{-1}$ VS $d^{-1}$) | | | | Statistical Information[a] | | |
|---|---|---|---|---|---|---|---|---|---|---|---|---|
| Cycle | Time (d) | C | Hst | H50 | H100 | C | Hst | H50 | H100 | C *vs.* Hst | C *vs.* H50 | C *vs.* H100 |
| 1st | 1 | 18.4 | 20.5 | 17.4 | 11.8 | 6.5 | 7.6 | 6.4 | 4.4 | a – a | a – a | a – a |
| | 3 | 29.5 | 48.9 | 47.7 | 54.5 | 2.0 | 5.3 | 5.6 | 8.0 | a – a | a – a | a – a |
| | 6 | 54.1 | 87.6 | 90.3 | 92.2 | 2.9 | 4.8 | 5.3 | 4.7 | a – b | a – b | a – b |
| 2nd | 1 | 13.0 | 17.5 | 33.3 | 29.3 | 4.6 | 6.6 | 13.0 | 11.3 | a – a | a – a | a – a |
| | 3 | 11.3 | 71.1 | 85.2 | 86.7 | −0.3 | 10.1 | 10.1 | 11.1 | a – b | a – b | a – b |
| | 6 | 51.9 | 91.3 | 95.0 | 95.3 | 4.8 | 2.5 | 1.3 | 1.1 | a – b | a – b | a – b |
| 3rd | 1 | 2.3 | 3.4 | −2.3 | 23.5 | 0.9 | 1.3 | −0.9 | 9.1 | a – a | a – a | a – b |
| | 3 | 26.6 | 32.2 | 63.2 | 70.8 | 4.9 | 5.5 | 12.2 | 9.1 | a – a | a – a | a – a |
| | 6 | 56.2 | 75.2 | 81.1 | 87.3 | 3.9 | 5.5 | 2.2 | 2.1 | a – b | a – b | a – b |
| Mean SDR[b] | | | | | | 3.3 | 5.3 | 5.6 | 5.8 | | | |

[a] Significant difference (*i.e.*, $p < 0.05$) occurs when two conditions do not share letters (*e.g.*, a – b). [b] The mean SDR was calculated over the 6 days of operation as an average of the three experimental cycles.

which $NO_2^-$ concentration was 4.30 mg $NO_2^-$ $L^{-1}$ (*i.e.*, 1.31 mg $NO_2^-$-N $L^{-1}$), similar to what was observed in the first two cycles of H100. Therefore, contrary to the first set of batch tests, $NO_2^-$ accumulated as a denitrification intermediate at the end of each test. Indeed, in the second set, each batch test was performed at a lower biomass percentage disadvantaging $NO_2^-$ reductase, which is more sensitive and slower than $NO_3^-$ reductase, and, thus, favouring $NO_2^-$ accumulation. As explained in section 3.1, in the presence of a higher biomass percentage, the endogenous HeDen denitrification rate was likely higher and contributed to further reducing $NO_2^-$ as well as $NO_3^-$ concentration. Considering the three cycles, the mean $NO_2^-$ concentration at the end of the $H_2$Den process reached the lowest value of 5.80 mg $L^{-1}$ (*i.e.*, 1.77 mg $NO_2^-$-N $L^{-1}$) for H100, whereas it was recorded at 7.70 (*i.e.*, 2.34 mg $NO_2^-$-N $L^{-1}$) and 6.90 mg $L^{-1}$ (*i.e.*, 2.10 mg $NO_2^-$-N $L^{-1}$) for Hst and H50, respectively. This trend suggests that further time is required to reduce $NO_2^-$, as well as a strategy to avoid $NO_2^-$ accumulation could be to increase the hydrogen supply to the system to raise the partial pressure of $H_2$ within the headspace of the batch reactors, thus promoting the solubilization of the electron donor and its immediate availability to the microorganisms.[40]

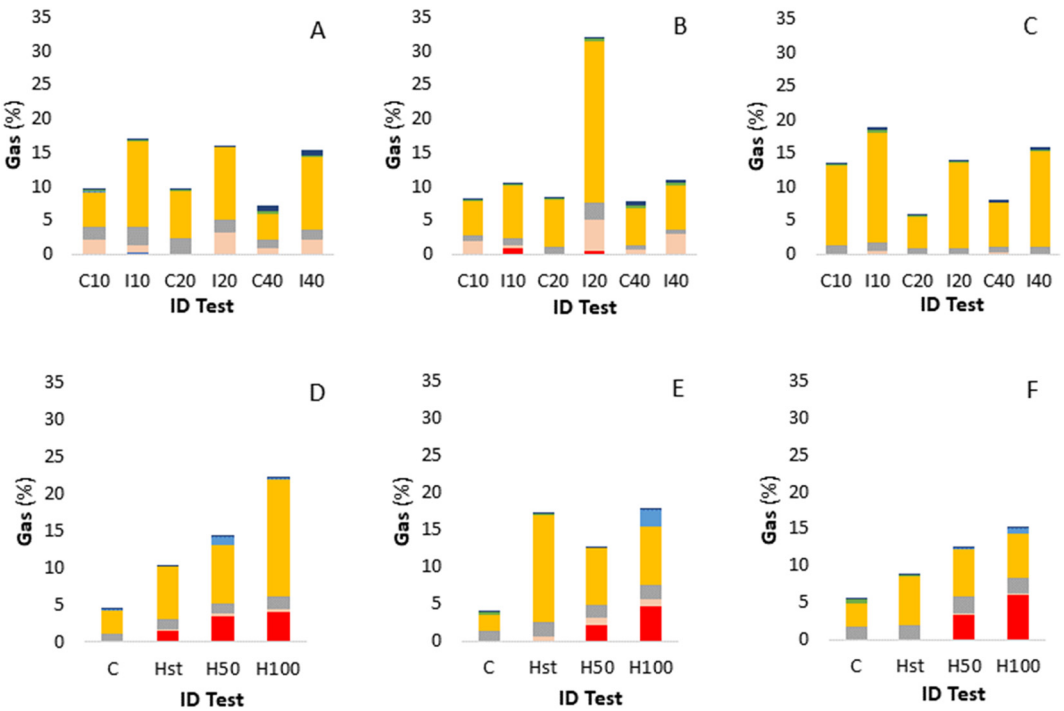


**Fig. 4** Gas composition (%) at the end of the hydrogenotrophic denitrification tests varying inoculum percentage (v/v) and hydrogen supply in the 1st (A and D), 2nd (B and E) and 3rd cycle (C and F): hydrogen (■), nitric oxide (■), methane (■), water (■), nitrogen (■), nitrous oxide (■) and carbon dioxide (■). The complement to 100% is represented by the argon gas used to flush the bottles at the beginning of the experiments.

 

### 3.3 Gaseous emissions and carbon utilisation at different inoculum percentages (v/v) and $H_2$ supply

The gas analyses enabled the evaluation of the release of gaseous denitrification intermediates (*i.e.*, NO, $N_2O$), besides verifying the presence of $N_2$, this being the final product of each biological denitrification process. $N_2O$ is a potent greenhouse gas in the troposphere and a stratospheric ozone depletion agent, whereas NO is an atmospheric pollutant as well as a precursor of tropospheric ozone,[41,42] besides being considered toxic to living organisms.[43] The gas composition at the end of each cycle for the first set of $H_2$Den tests, *i.e.*, studying the impact of the inoculum percentage, is shown in Fig. 4(panels A, B and C). The average $N_2O$ percentage (among the three cycles) was respectively 0.18, 0.20, and 0.26% for I10, I20, and I40 (Fig. 4A, B and C), with the background concentration detected in the air being approximately 0.04%. Therefore, a slight increase in $N_2O$ accumulation was observed with increasing inoculum percentage. To the best of the authors' knowledge, this is the first study reporting how $N_2O$ production from $H_2$Den changes at different inoculum percentages. Yan *et al.*[44] studied the effect of MLSS concentration on $N_2O$ emission in a nitrification/denitrification simultaneous process. It was noted that increasing the MLSS concentration from 1000 to 4000 mg $L^{-1}$ promoted $N_2O$ generation, reaching an average $N_2O$ emission rate of 2.1 μg $min^{-1}$ $g^{-1}$ of mixed liquor volatile suspended solids (MLVSS). In the present study, the $N_2O$ emission rates, calculated considering the 6 days of $H_2$Den operation, were considerably lower, reaching at most $4.03 \times 10^{-3}$ μg $min^{-1}$ $g^{-1}$ of AnGS in I10 (Table S4 – ESI† material). The $N_2O$ emission rate was $2.29 \times 10^{-3}$ μg $min^{-1}$ $g^{-1}$ of AnGS in I20 and $1.54 \times 10^{-3}$ μg $min^{-1}$ $g^{-1}$ of AnGS in I40.

Alternatively, the $N_2O$ release can be expressed on the basis of the total nitrogen removal. In the present study, the $N_2O$ percentage, calculated as mg $N_2O$-N produced/mg total nitrogen removed,[45] increased from 2.65 to 3.66% with the increment in the inoculum percentage (v/v) (Table S4 – ESI† material). These values are notably lower than what was previously observed in HeDen experiences, in which $N_2O$ can reach up to 13%.[20] Indeed, in this study, the highest $N_2O$ percentage of 12.09% was observed in the control tests in which endogenous HeDen occurred. Commonly, a low pH during the denitrification process can enhance the risk of $N_2O$ emission, but the $H_2$Den process produces alkalinity, avoiding pH decrease and, thus, limiting $N_2O$ emissions.[45] In the first set of experiments, the measured pH ranged from 7.6 to 8.9 (Fig. S2 – ESI† material), indicating a net alkalinity production according to Ex.[1]

As regards NO, its percentage was null in the inoculum percentage tests, while it reached at most 0.03 and 0.15% in I10 and I20, respectively (Fig. 4A, B and C).

Fig. 4(panels A, B and C) shows that the residual $H_2$ was negligible in the inoculum percentage tests, suggesting that $H_2$ was effectively solubilised and used by microorganisms.[46] $N_2$, *i.e.*, the final product of the denitrification process, was measured in percentages ranging between 6.5 and 23.6%, representing the main gaseous product. The high presence of $N_2$ indicates that the denitrification reaction was completed.[47] It can be observed that, in control tests, the $N_2$ percentage is constantly lower than in the corresponding inoculum percentage test, confirming that the use of $H_2$ as an inorganic electron donor allowed a more complete denitrification.[33]

In the inoculum percentage tests, $CH_4$ was also observed in the headspace, reaching 4.7% at most (Fig. 4). The AnGS used in the present study was collected from an UASB reactor used to treat dairy wastewater for $CH_4$ production.[39] Thus, the presence of methanogenic microorganisms may have promoted $CH_4$ production during the start-up of the experiments[48] in the presence of available organic matter under anoxic conditions.[32] Nevertheless, at the end of the 3rd cycle, $CH_4$ percentages were constantly below 0.5%, suggesting that the $CH_4$ production observed in the previous cycles was due to residual easily hydrolysable organic matter present in the original AnGS. Indeed, methanogens and denitrifiers may compete for organic carbon sources,[49] with methanogens likely being favoured in the first set of experiments due to pH values (Fig. S2 – ESI† materials) falling close to the optimal pH range for methane production in the first days of observation, *i.e.*, 6.8–7.5.[48] Eventually, the $CO_2$ percentage reached 0.8% at most, in accordance with previous studies investigating denitrification processes.[50]

Fig. 4(panels D, E and F) shows that the $N_2O$ percentages observed in the $H_2$Den tests were lower than in the first sets. In particular, $N_2O$ reached 0.13% in the Hst test, being slightly lower than the percentages detected in the I10, I20 and I40 tests. In Hst, the accumulation of intermediates in the liquid and gaseous phase (*i.e.*, $NO_2^-$ and $N_2O$, respectively) was likely due to the scarce availability of $H_2$, as also confirmed by the negligible percentage of residual $H_2$ at the end of the test (Fig. 4D, E and F). On the other hand, $N_2O$ production expressed as percentage in the headspace was notably lower in H50 and H100, *i.e.*, 0.02% (Table S4†). Besides, the lowest $N_2O$ emission rate of $4.88 \times 10^{-4}$ μg $min^{-1}$ $g^{-1}$ of AnGS was reached in H100. Therefore, the $N_2O$ percentages were similar when $H_2$ was supplied in excess compared to the stoichiometry. Similarly, Li *et al.*[27] observed that $N_2O$ accumulation was comparable at various dissolved hydrogen concentrations. In the H50 and H100 conditions, the leftover $H_2$ in the headspace suggests that further time would have been necessary to solubilise $H_2$ and complete the denitrification reaction. Indeed, in the H50 and H100 tests, the leftover $H_2$ reached up to 3.4 and 6.0%, respectively (Fig. 4D, E and F). This result suggests that part of the $H_2$ remained inside the system due to the supply in excess, thus establishing a new liquid–gas equilibrium condition between dissolved and gaseous $H_2$. As previously discussed, $H_2$ accumulation in the headspace can limit $NO_2^-$ removal, the electron donor being less available for microorganisms. Thus, the leftover $H_2$ can explain the residual $NO_2^-$ observed in the $H_2$ supply tests. A possible solution to this drawback may be

the implementation of an $H_2$ recirculation in the AnGS $H_2$Den process, which could enhance $H_2$ solubilisation,[51] likely increasing further $H_2$ availability for microorganisms and, therefore, $NO_2^-$ removal.

In the $H_2$ supply tests (Fig. 4D, E and F), the $N_2$ percentage ranged between 2.1% (in the control of the 2nd cycle) and 15.8% (in the H100 condition of the 1st cycle). Similar to n- was observed in the first set of experiments, $N_2$ was the dominant outlet gas, indicating the effectiveness of the denitrification reaction. $CH_4$ percentage was constantly below 0.9%, indicating that methanogens decreased their activity with respect to the first set of experiments. Indeed, in the 3rd cycle of the $H_2$ supply tests, $CH_4$ was null. $CO_2$ production was negligible, whereas NO was observed in very low percentages, except for H50 in the 1st cycle and for H100 in the 2nd cycle, in which NO percentages were 1.21 and 2.32%, respectively. Under these two conditions, in the intermediate days, $NO_2^-$-N concentrations were considerably high, *i.e.*, 6.85 and 13.48 mg $NO_2^-$-N $L^{-1}$, respectively. Thus, the $NO_2^-$ reduction observed from day 3 to day 6 may have promoted NO accumulation.[52]

## 4 Conclusion

The AnGS $H_2$Den process was investigated in two sets of experimental tests focusing on evaluating the impact of inoculum percentage and $H_2$ supply on denitrification. A NRE up to 95.8% was reached with a 10% (v/v) inoculum percentage, which likely promoted $H_2$Den over endogenous HeDen. Furthermore, a 10% (v/v) inoculum percentage ensured the maximal average specific denitrification rate of 6.0 mg $NO_3^-$ $g^{-1}$ VS $d^{-1}$. A 100% excess (with respect to the stoichiometry) in $H_2$ supply limited the residual $NO_2^-$ concentration compared to stoichiometric and 50% $H_2$ excess. The $N_2O$ percentage in the headspace reached approximately 0.20%, regardless of the initial $H_2$ supply, and NO and $CO_2$ releases were negligible. Therefore, greenhouse gas production was significantly lower than in HeDen processes. Besides, the low organic carbon released from granules could make the process appealing for drinking water production. Next steps to exploit the full potential of AnGS $H_2$Den should focus on the implementation of the process in semicontinuous and continuous mode while also investigating specific reactor configurations designed to preserve the original shape of the granules, *e.g.* an UASB reactor, eventually reinforced by gas recirculation to sustain a higher $H_2$ solubilisation.

## Data availability

The data supporting this article have all been included in the manuscript and in the ESI.†

## Author contributions

E. Marino: conceptualization, data curation, formal analysis, investigation, validation, visualization, writing – original draft, writing – review & editing. A. Oliva: conceptualization, supervision, validation, writing – review & editing. S. Papirio: conceptualization, project administration, supervision, resources, writing – review & editing. G. Esposito: resources, supervision, writing – review & editing. F. Pirozzi: funding acquisition, project administration, resources, supervision, writing – review & editing.

## Conflicts of interest

The authors declare that they have no known competing financial interests or personal relationships that could have appeared to influence the work reported in this paper.

## Acknowledgements

The Ph.D. scholarship of Emanuele Marino was co-funded by the Italian Ministry of University and Scientific Research, within the Mission 4 of Piano Nazionale di Ripresa e Resilienza (PNRR) as regulated by the Ministry Decree 352/2022, and by the company Acqua Campania SpA.

## References

1 Stockholm International Water Institute (SIWI), UNICEF. Water Scarcity and Climate Change Enabling Environment Analysis for WASH: Middle East and North Africa, 2023, Available from: **https://siwi.org/publications/water-scarcity-and-climate-change-enabling-environment-for-wash/**.

2 A. A. Salehi, M. Ghannadi-Maragheh, M. Torab-Mostaedi, R. Torkaman and M. Asadollahzadeh, A review on the water-energy nexus for drinking water production from humid air, *Renewable Sustainable Energy Rev.*, 2020, 120, DOI: **10.1016/j.rser.2019.109627**.

3 R. Picetti, M. Deeney, S. Pastorino, M. R. Miller, A. Shah and D. A. Leon, *et al.*, Nitrate and nitrite contamination in drinking water and cancer risk: A systematic review with meta-analysis, *Environ. Res.*, 2022, 210, DOI: **10.1016/j.envres.2022.112988**.

4 N. Gruber and J. N. Galloway, An Earth-system perspective of the global nitrogen cycle, *Nature*, 2008, **451**(7176), 293–296, Available from: **https://www.nature.com/articles/nature06592**.

5 E. Abascal, L. Gómez-Coma, I. Ortiz and A. Ortiz, Global diagnosis of nitrate pollution in groundwater and review of removal technologies, *Sci. Total Environ.*, 2022, 810, Available from: **https://linkinghub.elsevier.com/retrieve/pii/S0048969721073095**.

6 M. F. Carboni, S. Mills, S. Arriaga, G. Collins, U. Z. Ijaz and P. N. L. Lens, Autotrophic denitrification of nitrate rich wastewater in fluidized bed reactors using pyrite and elemental sulfur as electron donors, *Environ. Technol. Innovation*, 2022, 28, DOI: **10.1016/j.eti.2022.102878**.

7 S. Singh, A. G. Anil, V. Kumar, D. Kapoor, S. Subramanian and J. Singh, *et al.*, Nitrates in the environment: A critical review of their distribution, sensing techniques, ecological effects and remediation, *Chemosphere*, 2022, 287, DOI: **10.1016/j.chemosphere.2021.131996**.

 

8 G. Zou, S. Papirio, A. Ylinen, F. Di Capua, A. M. Lakaniemi and J. A. Puhakka, Fluidized-bed denitrification for mine waters. Part II: Effects of Ni and Co, *Biodegradation*, 2014, **25**(3), 417–423, DOI: **10.1016/j.cej.2015.09.074**.

9 G. Yu, J. Wang, L. Liu, Y. Li, Y. Zhang and S. Wang, The analysis of groundwater nitrate pollution and health risk assessment in rural areas of Yantai, China, *BMC Public Health*, 2020, **20**(1), 437, Available from: **https://bmcpublichealth.biomedcentral.com/articles/10.1186/s12889-020-08583-y**.

10 M. Ward, R. Jones, J. Brender, T. De Kok, P. Weyer and B. Nolan, *et al.*, Drinking Water Nitrate and Human Health: An Updated Review, *Int. J. Environ. Res. Public Health*, 2018, **15**(7), 1557, Available from: **https://www.mdpi.com/1660-4601/15/7/1557**.

11 T. H. Le-Lam, H. H. Lam, H. P. Phan, T. Nguyen and T. Dang-Bao, Thioglycolic acid-functionalized gold nanoparticles: Capping agent-affected color perception stability towards nitrate sensing purpose, *Mater. Today: Proc.*, 2022, **66**, 2720–2725, DOI: **10.1016/j.matpr.2022.06.502**.

12 M. Zhou, W. Wang and M. Chi, Enhancement on the simultaneous removal of nitrate and organic pollutants from groundwater by a three-dimensional bio-electrochemical reactor, *Bioresour. Technol.*, 2009, **100**(20), 4662–4668, DOI: **10.1016/j.biortech.2009.05.002**.

13 F. Rezvani, M.-H. Sarrafzadeh, S. Ebrahimi and H.-M. Oh, Nitrate removal from drinking water with a focus on biological methods: a review, *Environ. Sci. Pollut. Res.*, 2019, **26**(2), 1124–1141, Available from: **https://link.springer.com/10.1007/s11356-017-9185-0**.

14 X. Wang, L. Xing, T. Qiu and M. Han, Simultaneous removal of nitrate and pentachlorophenol from simulated groundwater using a biodenitrification reactor packed with corncob, *Environ. Sci. Pollut. Res.*, 2013, **20**(4), 2236–2243, Available from: **https://link.springer.com/10.1007/s11356-012-1092-9**.

15 Y. Liu, H. H. Ngo, W. Guo, L. Peng, X. Chen and D. Wang, *et al.*, Modelling electron competition among nitrogen oxides reduction and $N_2O$ accumulation in hydrogenotrophic denitrification, *Biotechnol. Bioeng.*, 2018, **115**(4), 978–988, Available from: **https://onlinelibrary.wiley.com/doi/10.1002/bit.26512**.

16 H. Chen, L. Zeng, D. Wang, Y. Zhou and X. Yang, Recent advances in nitrous oxide production and mitigation in wastewater treatment, *Water Res.*, 2020, **184**, 116168, Available from: **https://linkinghub.elsevier.com/retrieve/pii/S0043135420307053**.

17 Y. Chen, L. Zhang, L. Ding, Y. Zhang, X. Wang and X. Qiao, *et al.*, Sustainable treatment of nitrate-containing wastewater by an autotrophic hydrogen-oxidizing bacterium, *Environ. Sci. Ecotechnology*, 2022, 9, DOI: **10.1016/j.ese.2022.100146**.

18 F. Di Capua, F. Pirozzi, P. N. L. Lens and G. Esposito, Electron donors for autotrophic denitrification, *Chem. Eng. J.*, 2019, **362**(3), 922–937, DOI: **10.1016/j.cej.2019.01.069**.

19 N. Sunger and P. Bose, Autotrophic denitrification using hydrogen generated from metallic iron corrosion, *Bioresour. Technol.*, 2009, **100**(18), 4077–4082, DOI: **10.1016/j.biortech.2009.03.008**.

20 S. Wang, Y. Wang, P. Li, L. Wang, Q. Su and J. Zuo, Development and characterizations of hydrogenotrophic denitrification granular process: Nitrogen removal capacity and adaptability, *Bioresour. Technol.*, 2022, 363, DOI: **10.1016/j.biortech.2022.127973**.

21 K. Kiskira, S. Papirio, C. Fourdrin, E. D. van Hullebusch and G. Esposito, Effect of Cu, Ni and Zn on Fe(II)-driven autotrophic denitrification, *J. Environ. Manage.*, 2018, **218**, 209–219, DOI: **10.1016/j.jenvman.2018.04.050**.

22 P. Nikolaidis and A. Poullikkas, A comparative overview of hydrogen production processes, *Renewable Sustainable Energy Rev.*, 2017, **67**, 597–611, DOI: **10.1016/j.rser.2016.09.044**.

23 P. Li, Y. Wang, J. Zuo, R. Wang, J. Zhao and Y. Du, Nitrogen Removal and $N_2O$ Accumulation during Hydrogenotrophic Denitrification : Influence of Environmental Factors and Microbial Community Characteristics, *Environ. Sci. Technol.*, 2017, **51**(2), 870–920, DOI: **10.1016/j.jenvman.2018.04.050**.

24 Z. Bi, Q. Zhang, X. Xu, Y. Yuan, N. Ren and D. J. Lee, *et al.*, Perspective on inorganic electron donor-mediated biological denitrification process for low C/N wastewaters, *Bioresour. Technol.*, 2022, 363, DOI: **10.1016/j.biortech.2022.127890**.

25 S. Mills, A. Christine, M. Prevedello, V. J. De, V. O. Flaherty and P. N. L. Lens, *et al.*, Unifying concepts in methanogenic, aerobic, and anammox sludge granulation, *Environ. Sci. Ecotechnology*, 2024, 17, DOI: **10.1016/j.ese.2023.100310**.

26 S. J. Lim and T. H. Kim, Applicability and trends of anaerobic granular sludge treatment processes, *Biomass Bioenergy*, 2014, **60**, 189–202, DOI: **10.1016/j.biombioe.2013.11.011**.

27 P. Li, Y. Wang, J. Zuo, R. Wang, J. Zhao and Y. Du, Nitrogen removal and N2O accumulation during hydrogenotrophic denitrification: Influence of environmental factors and microbial community characteristics, *Environ. Sci. Technol.*, 2017, **51**(2), 870–879, DOI: **10.1016/j.jenvman.2018.04.050**.

28 M. Kumar, S. Matassa, F. Bianco, A. Oliva, S. Papirio and F. Pirozzi, *et al.*, Effect of Varying Zinc Concentrations on the Biomethane Potential of Sewage Sludge, *Water*, 2023, **15**(4), 1–11, DOI: **10.3390/w15040729**.

29 A. Oliva, L. C. Tan, S. Papirio, G. Esposito and P. N. L. Lens, Effect of methanol-organosolv pretreatment on anaerobic digestion of lignocellulosic materials, *Renewable Energy*, 2021, **169**, 1000–1012, DOI: **10.1016/j.renene.2020.12.095**.

30 R. Morello, F. Di Capua, G. Esposito, F. Pirozzi, U. Fratino and D. Spasiano, Sludge minimization in mainstream wastewater treatment: Mechanisms, strategies, technologies, and current development, *J. Environ. Manage.*, 2022, 319, DOI: **10.1016/j.jenvman.2022.115756**.

31 F. Di Capua, M. C. Mascolo, F. Pirozzi and G. Esposito, Simultaneous denitrification, phosphorus recovery and low sulfate production in a recirculated pyrite-packed biofilter (RPPB), *Chemosphere*, 2020, 255, DOI: **10.1016/j.chemosphere.2020.126977**.

32 A. Oliva, L. C. Tan, S. Papirio, G. Esposito and P. N. L. Lens, Fed-batch anaerobic digestion of raw and pretreated hazelnut skin over long-term operation, *Bioresour. Technol.*, 2022, 357, DOI: **10.1016/j.biortech.2022.127372**.

33 T. Tian and H. Yu, Denitrification with non-organic electron donor for treating low C/N ratio wastewaters, *Bioresour. Technol.*, 2020, 299, DOI: **10.1016/j.biortech.2019.122686**.

34 M. Chang, F. Fan, K. Zhang, Z. Wu, T. Zhu and Y. Wang, Denitrification performance and mechanism of a novel sulfur-based fiber carrier fixed-bed reactor: Co-existence of sulfur-based autotrophic denitrification and endogenous denitrification. Journal of Water, *Process Eng.*, 2023, 53, DOI: **10.1016/j.jwpe.2023.103618**.

35 J. Zhang, C. Fan, M. Zhao, Z. Wang, S. Jiang and Z. Jin, *et al.*, A comprehensive review on mixotrophic denitrification processes for biological nitrogen removal, *Chemosphere*, 2023, 313, DOI: **10.1016/j.chemosphere.2022.137474**.

36 T. Kobayashi, K.-Q. Xu and H. Chiku, Release of Extracellular Polymeric Substance and Disintegration of Anaerobic Granular Sludge under Reduced Sulfur Compounds-Rich Conditions, *Energies*, 2015, **8**(8), 7968–7985, Available from: **https://www.mdpi.com/1996-1073/8/8/7968**.

37 J. Wang, L. Xu, B. Huang, J. Li and R. Jin, Multiple electron acceptor-mediated sulfur autotrophic denitrification : Nitrogen source competition, long-term performance and microbial community evolution, *Bioresour. Technol.*, 2021, 329, DOI: **10.1016/j.biortech.2021.124918**.

38 R. Eamrat, Y. Tsutsumi, T. Kamei, W. Khanichaidecha, T. Ito and F. Kazama, Microbubble application to enhance hydrogenotrophic denitrification for groundwater treatment, *Environ. Nat. Resour. J.*, 2020, **18**(2), 156–165, Available from: **https://www.researchgate.net/publication/309266794_Hydrogenotrophic_Den**.

39 M. F. Carboni, A. P. Florentino, R. B. Costa, X. Zhan and P. N. L. Lens, Enrichment of Autotrophic Denitrifiers From Anaerobic Sludge Using Sulfurous Electron Donors, *Front. Microbiol.*, 2021, 12, DOI: **10.3389/fmicb.2021.678323**.

40 I. Keisar, C. Desitti, M. Beliavski, R. Epsztein, S. Tarre and M. Green, A pressurized hydrogenotrophic denitrification reactor system for removal of nitrates at high concentrations. Journal of Water, *Process Eng.*, 2021, 42, DOI: **10.1016/j.jwpe.2021.102140**.

41 H. Duan, Y. Zhao, K. Koch, G. F. Wells, M. Weißbach and Z. Yuan, *et al.*, Recovery of Nitrous Oxide from Wastewater Treatment: Current Status and Perspectives, *ACS ES&T Water*, 2021, **1**(2), 240–250, Available from: **https://pubs.acs.org/doi/10.1021/acsestwater.0c00140**.

42 S. Medinets, S. White, N. Cowan, J. Drewer, J. Dick and M. Jones, *et al.*, Impact of climate change on soil nitric oxide and nitrous oxide emissions from typical land uses in Scotland, *Environ. Res. Lett.*, 2021, **16**(5), 055035, Available from: **https://iopscience.iop.org/article/10.1088/1748-9326/abf06e**.

43 D. Richardson, H. Felgate, N. Watmough, A. Thomson and E. Baggs, Mitigating release of the potent greenhouse gas N2O from the nitrogen cycle – could enzymic regulation hold the key?, *Trends Biotechnol.*, 2009, **27**(7), 388–397, Available from: **https://linkinghub.elsevier.com/retrieve/pii/S0167779909000924**.

44 X. Yan, D. Guo, D. Qiu, S. Zheng, M. Jia and M. Zhang, *et al.*, Effect of mixed liquor suspended solid concentration on nitrous oxide emission from an anoxic/oxic sequencing bioreactor, *Desalin. Water Treat.*, 2019, **163**, 48–56, Available from: **https://linkinghub.elsevier.com/retrieve/pii/S1944398624170300**.

45 Y. Wang, P. Li, J. Zuo, Y. Gong, S. Wang and X. Shi, *et al.*, Inhibition by free nitrous acid (FNA) and the electron competition of nitrite in nitrous oxide ($N_2O$) reduction during hydrogenotrophic denitrification, *Chemosphere*, 2018, **213**, 1–10, DOI: **10.1016/j.chemosphere.2018.08.135**.

46 D. Chen, H. Wang, B. Ji, K. Yang, L. Wei and Y. Jiang, A high-throughput sequencing study of bacterial communities in an autohydrogenotrophic denitrifying bio-ceramsite reactor, *Process Biochem.*, 2015, **50**(11), 1904–1910, DOI: **10.1016/j.procbio.2015.07.006**.

47 W. Zhou, Y. Sun, B. Wu, Y. Zhang, M. Huang and T. Miyanaga, *et al.*, Autotrophic denitrification for nitrate and nitrite removal using sulfur-limestone, *J. Environ. Sci.*, 2011, **23**(11), 1761–1769, DOI: **10.1016/S1001-0742(10)60635-3**.

48 S. Pau, L. C. Tan and P. N. L. Lens, Effect of pH on lactic acid fermentation of food waste using different mixed culture inocula, *J. Chem. Technol. Biotechnol.*, 2022, **97**(4), 950–961, Available from: **https://onlinelibrary.wiley.com/doi/10.1002/jctb.6982**.

49 X. Wu, C. Wang, D. Wang, Y. X. Huang, S. Yuan and F. Meng, Simultaneous methanogenesis and denitrification coupled with nitrifying biofilm for high-strength wastewater treatment: Performance and microbial mechanisms, *Water Res.*, 2022, 225, DOI: **10.1016/j.watres.2022.119163**.

50 X. Fu, R. Hou, P. Yang, S. Qian, Z. Feng and Z. Chen, *et al.*, Application of external carbon source in heterotrophic denitri fi cation of domestic sewage: A review, *Sci. Total Environ.*, 2022, 817, DOI: **10.1016/j.scitotenv.2022.153061**.

51 K. A. Karanasios, I. A. Vasiliadou, S. Pavlou and D. V. Vayenas, Hydrogenotrophic denitrification of potable water: A review, *J. Hazard. Mater.*, 2010, **180**(1–3), 20–37, DOI: **10.1016/j.jhazmat.2010.04.090**.

52 L. Lan, J. Zhao, S. Wang, X. Li, L. Qiu and S. Liu, *et al.*, NO and N2O accumulation during nitrite-based sulfide-oxidizing autotrophic denitrification, *Bioresour. Technol. Rep.*, 2019, 7, DOI: **10.1016/j.biteb.2019.100190**.

 